STROJNÍCKY ČASOPIS

ČASOPIS PRE PROBLÉMY MECHANIKY V STROJNÍCTVE

ROČNÍK 42 1991 ČÍSLO 2

Bifurcation, periodic and chaotic orbits of the two-body non-linear mechanical system

J. AWREJCEWICZ

Dimensionless nonlinear differential equations with periodically changing coefficients governing the dynamics of a rotor with rectangular cross-section fixed in rigid bearings of a rigid frame are analyzed. The use of the Newton – Raphson procedure as well as the sooting method has made it possible (with a high calculation accurracy) to observe the periodic orbits changes accompanying the changes of chosen parameters, with a simultaneous tracing of the values of the multipliers. The latter are decisive for the stability and bifurcation of the considered periodic orbits. Two different scenarious leading from periodic to chaotic orbits, which are not found in simple three-dimensional systems, are discussed and illustrated. Additionally the evolution of chaotic orbits during the change of a control parameter is observed.

Key words: Newton – Raphson method, characteristic multipliers, fundamental matrix, chaos, strange attractor

1. Introduction

The chaotic dynamics of simple nonlinear harmonically excited oscillators has been widely discussed (see for example [1, 2, 3]), where various methods of analyzing the transition from regular to irregular motion are shown. An specially useful method for tracing the periodic motions is the numerical method based on the solution of a boundary value problem using the shooting or Newton method or its modified version [4]. On the one hand, it makes it possible to calculate fixed points (periodic orbits) with great accuracy, and on the other, by means of simultaneous observation of the Floquet matrix eigenvalues, it enables us to obtain information concerning the stability and bifurcation of the periodic orbit considered. Moreover, the bifurcation points are accurately determined,

Dr. M. S. Eng. Jan Awrejcewicz, Technical University, Institute of Applied Mechanics, Stefanowskiego 1/5, 90-924 Lodz, Poland.

which in the case of the saddle-node bifurcation makes it possible to determine the critical parameter values, after passing which chaos appears.

The method was also used to observe the periodic orbit in a complex mechanical system with three degrees of freedom which is considered here. This kind of system was chosen for the following two reasons. The first has an application character and is reduced to the analysis of chaos in oscillating mechanical systems. The second has a cognitive aspect: It deals with the question if in complex physical systems there are transitions from periodic to chaotic motions different from those discovered in simple sinusoidally excited oscillators.

The analytical methods which lead to the discovery of chaotic orbits in simple anharmonic oscillators [5] seem to be or little or no use for the analysis of complex physical systems. Thence, in the present work the complex mechanical system is analyzed using numerical methods. Such an approach was used earlier with success for the analysis of single [6, 7] as well as coupled [8, 9] anharmonic oscillators.

2. The system analyzed

The diagram of the analyzed system is presented in Fig. 1 (the very similar system to this was considered earlier in [10]). A weightless rotor with the rectangular cross-section is fixed in a rigid bearings of a rigid frame 1. The frame, which can move only horizontally, is supported nonlinearly. Also the cylinder-like mass m, concentrated in the middle of the rotor, is nonlinearly supported in the x_2 direction.

The calculation model of the analyzed rotor is presented in Fig. 1b. The equations of motion of the rotor have the form:

$$\begin{aligned} m\ddot{x}_c &= -\xi_w k_\xi \cos \Phi - \eta_w k_\eta \sin \Phi, \\ m\ddot{y}_c &= \xi_w k_\xi \sin \Phi - \eta_w k_\eta \cos \Phi + mg, \\ I_z\ddot{\Phi} &= -M_0 + a(-\xi_w k_\xi \cos \Phi_0 + \eta_w k_\eta \sin \Phi_0). \end{aligned} \tag{1}$$

where:

x_c, y_c — coordinates of the center of mass of the cylinder,
I_z — mass moment of inertia of a cylinder with mass m in relation to the z axis,
ξ_w, η_w — coordinates of the point of puncture by the rotor in the coordinate system,
$O'\xi\eta$ — coordinate system whose axes are parallel to the main, central inertia axes of the cross section of the rotor,

k_ξ, k_η — rotor rigidities in the direction of the axes ξ and η,
M_0 — driving torque reduced by all the resistance torques,
a, Φ_0 — parameters characterising the position of the center of mass of the disk C in relation to the point of puncture of the rotor. For the states near the steady ones the torque M_0 is very small. Let

$$I_z = mi_s^2, \tag{2}$$

where i_s is the inertia radius, then the third equation of (1) will assume the form

$$\ddot{\Phi} = \frac{a}{mi_s^2}(-\xi_w k_\xi \cos \Phi_0 + \eta_w k_\eta \sin \Phi_0). \tag{3}$$

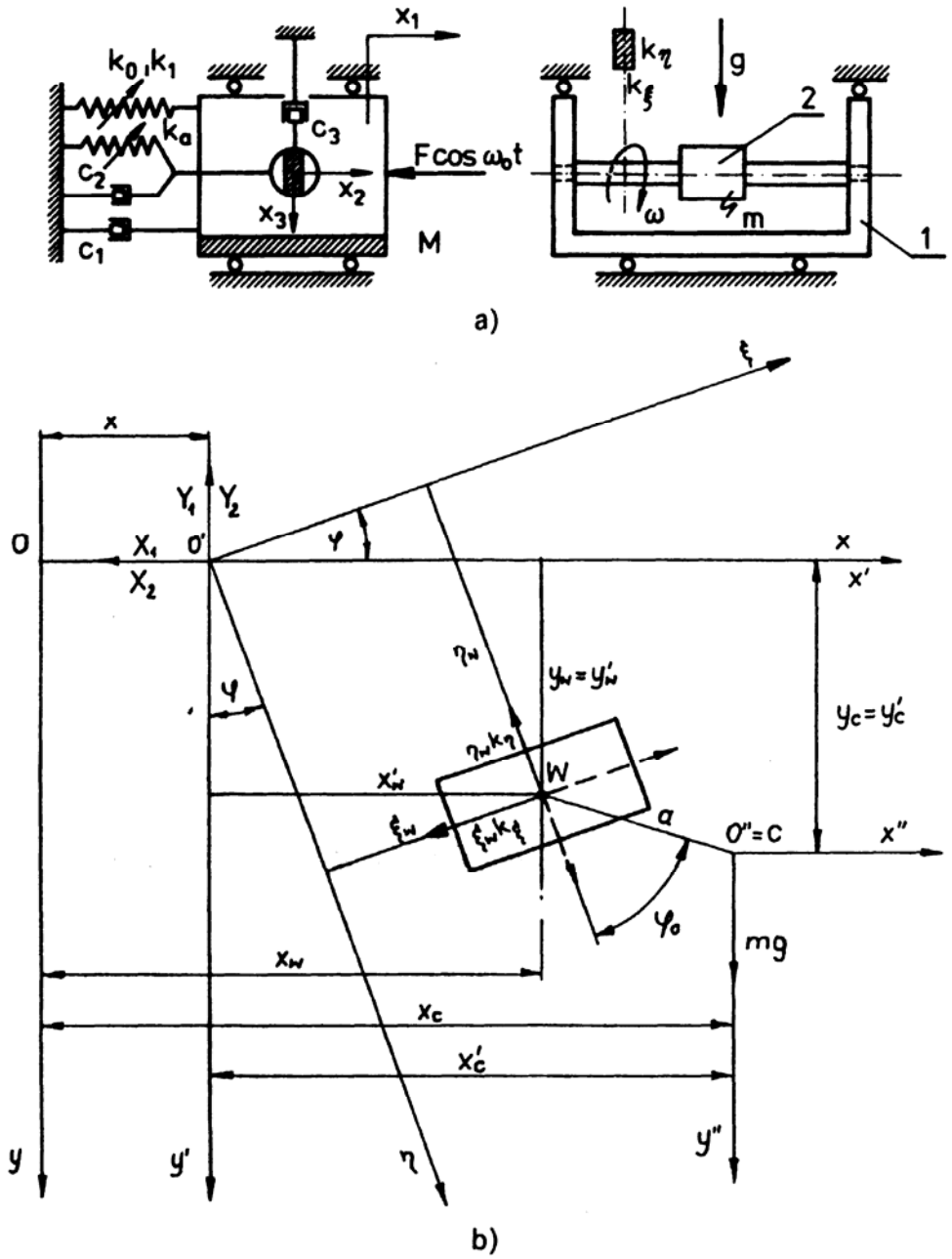

Fig. 1. The analyzed system (a)) and a calculation diagram of the rotor (b))

As the excentricity a and the rotor deflection ξ_w and η_w are small as compared to the inertia radius, then we obtain

$$\ddot{\Phi} = 0, \ \dot{\Phi} = \omega = \text{const}, \ \Phi = \omega t . \tag{4}$$

The following geometric dependences result from the Fig. 1b:

$$\begin{aligned} \xi_w &= (x_w - x)\cos\Phi + y_w \sin\Phi, \\ \eta_w &= (x_w - x)\sin\Phi - y_w \cos\Phi, \\ y_c &= y_w + a\cos(\Phi + \Phi_0), \\ x_c &= x_w + a\sin(\Phi + \Phi_0), \end{aligned} \tag{5}$$

where x_w, y_w are the coordinates of the point of puncture by the rotor W in the system Oxy.

In order to write down the equations of motion of the mass M it is necessary to determine the dynamic reactions on the rotor in its points of support. They are determined from the equations

$$\begin{aligned} X_1 + X_2 + \xi_w k_\xi \cos\omega t + \eta_w k_\eta \sin\omega t = 0, \\ Y_1 + Y_2 - \xi_w k_\xi \sin\omega t + \eta_w k_\eta \cos\omega t = 0, \end{aligned} \tag{6}$$

where X_1, Y_1 and X_2, Y_2 denote the support reactions on the left and right end of the rotor, respectively.

After assuming that $x = x_1$, $x_w = x_2$, $y_w = x_3$ and additionally that the force $F_x = k_a x_2$ is acting on the mass m in the x_2 direction the following governing equations are obtained

$$M\ddot{x}_1 + c_1\dot{x}_1 - k_0 x_1 + k_1 x_1^3 + \left\{\frac{k_\xi + k_\eta}{2} + \frac{k_\xi - k_\eta}{2}\cos 2\omega t\right\} x_1 -$$

$$- \left\{\frac{k_\xi + k_\eta}{2} + \frac{k_\xi - k_\eta}{2}\cos 2\omega t\right\} x_2 + \frac{k_\xi - k_\eta}{2} x_3 \sin 2\omega t = F\cos\omega_0 t,$$

$$m\ddot{x}_2 + c_2\dot{x}_2 - \left\{\frac{k_\xi + k_\eta}{2} + \frac{k_\xi - k_\eta}{2}\cos 2\omega t\right\} x_1 +$$

$$+ \left\{\frac{k_\xi + k_\eta}{2} + \frac{k_\xi - k_\eta}{2}\cos 2\omega t\right\} x_2 - k_a x_2 - \frac{k_\xi - k_\eta}{2} x_3 \sin 2\omega t =$$

$$= ma\omega^2 \sin(\omega t + \phi_0),$$

$$m\ddot{x}_3 + c_3\dot{x}_3 + \frac{k_\xi - k_\eta}{2} x_1 \sin 2\omega t - \frac{k_\xi - k_\eta}{2} x_2 \sin 2\omega t +$$

$$+ \left\{\frac{k_\xi + k_\eta}{2} - \frac{k_\xi - k_\eta}{2} \cos 2\omega t\right\} x_3 = ma\omega^2 \cos(\omega t + \Phi_0) + mg,$$

$$k_a = r\left\{\frac{k_\xi + k_\eta}{2} + \frac{k_\xi - k_\eta}{2} \cos 2\omega t\right\} - k_2 x_2^2, \tag{7}$$

where x_1 — horizontal displacement of the base; x_2, x_3 — horizontal and vertical displacement of the concentrated mass m situated in the middle of rotor length; M — base mass; k_0, k_1 — stiffnesses connecting the base with a motionless system; ω — frequency of the rotor revolutions; F and ω_0 — amplitude and external forcing frequency; c_1, c_2, c_3 — viscotic damping; g — acceleration of gravitation; k_2 — Duffing-type stiffness; r — amplification coefficient. The force F_x can be realized, for example, by induction of a electromagnetic field. Examples of chaotic behaviour in the systems with a Duffing type stiffness of the form $-k_0x_1 + k_1x_1^3$ are considered in a book by Thompson and Stewart [2].
Thanks to the relations given below

$$\tau = (k_0 M^{-1})^{\frac{1}{2}} t, \qquad y_1 = (k_1 k_0^{-1})^{\frac{1}{2}} x_1, \qquad x_2 = \frac{2mgy_3}{k_\xi + k_\eta},$$

$$x_3 = \frac{2mgy_5}{k_\xi + k_\eta}, \qquad z = \frac{k_\xi + k_\eta}{2}, \qquad b = \frac{k_\xi - k_\eta}{2k_0},$$

$$d_1 = c_1 (k_0 M)^{\frac{-1}{2}}, \qquad e = mg(k_1 k_0^{-3})^{\frac{1}{2}}, \qquad \nu = \omega(Mk_0^{-1})^{\frac{1}{2}},$$

$$\mu = mM^{-1}, \qquad q = F(k_1 k_0^{-3})^{\frac{1}{2}} \qquad \nu_0 = \omega_0 (Mk_0^{-1})^{\frac{1}{2}},$$

$$q_1 = \omega^2 a g^{-1} \cos \Phi_0, \qquad q_2 = \omega^2 a g^{-1} \sin \Phi_0, \qquad d_2 = \frac{2c_2 (k_0 M^{-1})^{\frac{1}{2}}}{(k_\xi + k_\eta)},$$

$$d_3 = \frac{2c_3 (k_0 M^{-1})^{\frac{1}{2}}}{(k_\xi + k_\eta)}, \qquad \gamma = 8k_2 m^2 g^2 (k_\xi + k_\eta)^{-3}, \qquad \frac{\mathrm{d}}{\mathrm{d}\tau} = ',$$

$$\varepsilon = \frac{b}{z} = \frac{k_\xi - k_\eta}{k_\xi + k_\eta}, \tag{8}$$

the following nondimensional set of equations is obtained

$$y_1' = y_2,$$

$$y_2' = (1 - z)y_1 - y_1^3 - by_1 \cos 2\nu\tau - d_1 y_2 + ey_3(1 + \varepsilon \cos 2\nu\tau) - \\ - \varepsilon e y_5 \sin 2\nu\tau + q \cos \nu_0 \tau,$$

$$y_3' = y_4,$$

$$y_4' = \frac{z}{\mu}\left\{\frac{z}{e} y_1(1 + \varepsilon \cos 2\nu\tau) + ry_3(1 + \varepsilon \cos 2\nu\tau) + \right.$$

$$\left. + \varepsilon y_5 \sin 2\nu\tau - d_2 y_4 - \gamma y_3^3 + q_1 \sin \nu\tau + q_2 \cos \nu\tau\right\},$$

$$y_5' = y_6,$$

$$y_6' = \frac{z}{\mu}\left\{-\frac{z}{e} \varepsilon y_1 \sin 2\nu\tau + \varepsilon y_3 \sin 2\nu\tau - y_5(1 - \varepsilon \cos 2\nu\tau) - \right.$$

$$\left. - d_3 y_6 + 1.0 + q_1 \cos \nu\tau + q_2 \sin \nu\tau\right\}. \qquad (9)$$

3. The method

The periodic orbit of the equation system (9) have been traced on the basis of solving the boundary value problem (the integration of the differential equations has been made on the basis of the Gear method [11]). The idea of the method consists in the construction of the mapping $M(y^{(k)}) = M^{(k)}$, while the distance between two arbitrary consecutive points in the case of nonautonomous systems analysis is equal to the period of the sought solution. The error $E = y^{(k)} - M^{(k)}$ shows the accuracy of the estimation (k). Thanks to the shooting method and the Newton–Raphson procedure we can look for the values of E. The calculations are interrupted if $|E| \leq 10^{-5}$.

The analysis of stability of the found periodic solutions is reduced to the analysis of linear differential equation systems with the periodic coefficients

$$\Delta \boldsymbol{p}' = \boldsymbol{J}(\tau)\Delta \boldsymbol{p} = \left(\frac{\partial \boldsymbol{y}'}{\partial \boldsymbol{y}}\right)_{y_p(\tau)} \Delta \boldsymbol{p}, \qquad (10)$$

where $\boldsymbol{J}(\tau + \boldsymbol{T}) = \boldsymbol{J}(\tau)$ and $\Delta \boldsymbol{p}$ is a perturbation vector of the investigated periodic solution $\acute{\boldsymbol{y}}_p(\tau)$.

According to the Floquet theory, the general solution of (10) is

$$\Delta \boldsymbol{p} = \Phi(\tau)\Delta \boldsymbol{p}\,(\mathbf{0}), \tag{11}$$

where $\Phi(\tau) = \Phi(\tau + \boldsymbol{T})$ is the fundamental matrix. The eigenvalues of the matrix $\Phi(\boldsymbol{T}) = \partial \boldsymbol{M}/\partial \boldsymbol{y}$, which are the multipliers, are known from the iteration mentioned above as the Jacobi matrix of the point mapping at the fixed point.

The multipliers determine the stability and bifurcation of the considered periodic orbit. In the case when one of the multipliers is real and crosses the unit circle of the complex plane at the point -1 in the direction outside the circle, the considered periodic orbit becomes unstable. A new orbit with a two times greater period branches from it.

In the case when the transition conditions given above are retained, if one of the multipliers exceeds the value of $+1$, then the considered periodic orbit becomes unstable and either an orbit with its period two times smaller or a chaotic orbit appears.

The last of the classical cases has its place when a pair of complex conjugate characteristic multipliers crosses the unit circle of the complex plane. In this case a new periodic or quasiperiodic solution can appear [12].

4. Two different routes to chaos

Let us consider the behaviour of the system accompanying the change of b for the following constant parameters: $z = 0.1$, $d_1 = 0.4$, $\mu = 0.1$, $\nu = \nu_0 = 0.7$, $q = 0.5$, $q_1 = q_2 = 0.0$, $e = 0.1$, $d_2 = d_3 = 0.1$, $r = \gamma = 0.5$.

A periodic orbit with the period $2\pi/\nu_0$, found for the value of $b = 0.00001$ (Fig. 2) has been chosen as the starting point. As the oscillations of the coordinate y_5 are negligibly small as compared with the other coordinates on account of the small value of b, they have been omitted from Fig. 2. Next, the orbit has been traced with the increase of b by means of the method described in the previous section. The calculation results are shown in Fig. 3. The curves presented there are a set of constant points of Poincarè mapping (presentation is reduced to the projections of y_1, y_3 and y_5, while the dashed line shows the unstable solutions. The point -1 is a period-doubling type bifurcation point.

The newly found periodic solution with the period $4\pi/\nu_0$ is an unstable one. For $b = 0.02$ it is shown in Fig. 4. As for $b = 0.02$ the smallest characteristic multiplier has the value of -4.06, and it further decreases with the increase of b, reaching the value of -15.7 for $b = 0.03625$, further tracing of the orbit has

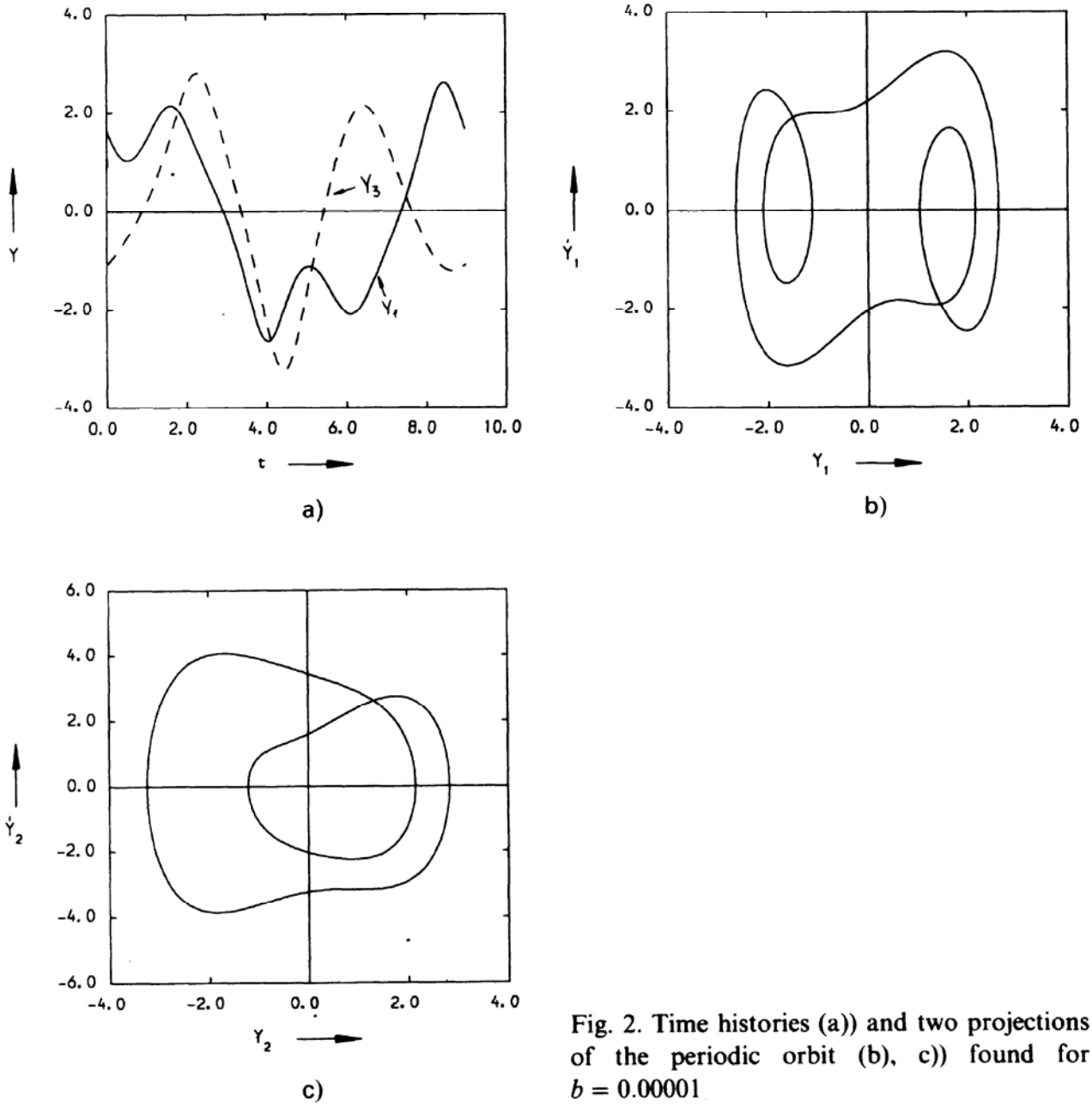

Fig. 2. Time histories (a)) and two projections of the periodic orbit (b), c)) found for $b = 0.00001$

been neglected on account of the weakening convergence of the Newton – Raphson method for such an unstable solution.

The periodic orbit with the period $2\pi/\nu_0$ has been traced for the value of $b = 0.075$. For this value of b one of the multipliers has reached the value of $+1$, and the further increase of b has resulted in the disappearance of the periodic orbit, and the appearance of the chaotic orbit. Two projections of such an orbit for $b = 0.1$ are presented in Fig. 5 (projection $y_2(y_3)$ stands for the trajectory of the concentrated mass fixed in the center of the rotor).

The periodic orbit presented in Fig. 2 can also be observed with the change of another parameter. We shall show, choosing q for the bifurcation parameter, that chaotic motión also appears with its decrease, but the scenario leading to

the chaotic motion is totally different from that presented before. The results of periodic orbit tracing with the change of q are presented in Fig. 6 where (similary to Fig. 3) projections y_1 and y_3 are shown. For $q = 4.55$ one of multipliers exceeds the value of -1, the solution with the period $2\pi/\nu_0$ becomes unstable, and a new solution branches from it, with the period $4\pi/\nu_0$. Two projections of the solution for $q = 4.53$ are presented in Fig. 7. It appears that this solution

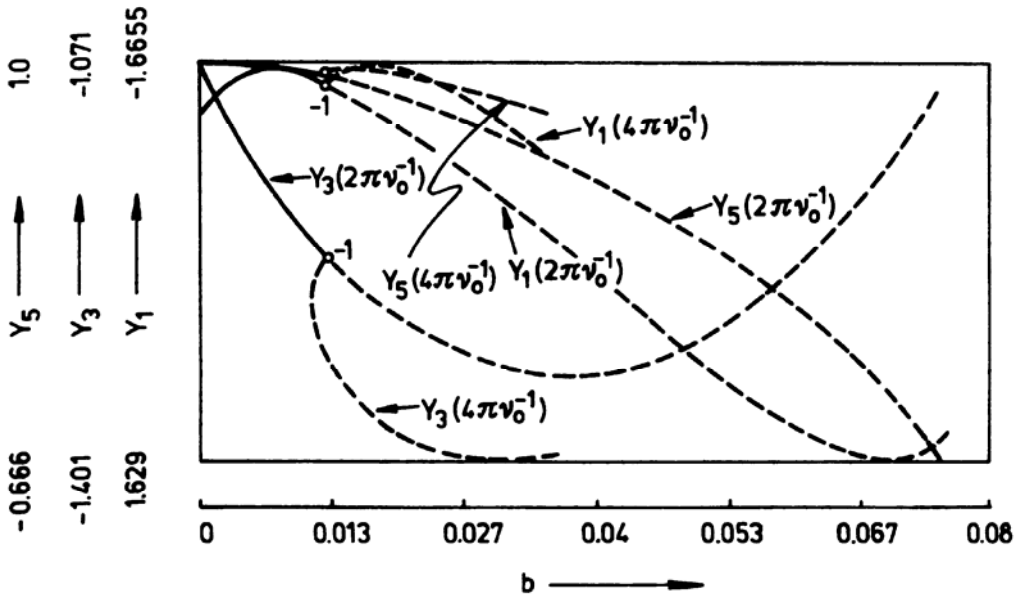

Fig. 3. Solution branches and bifurcation points of the periodic orbit against b

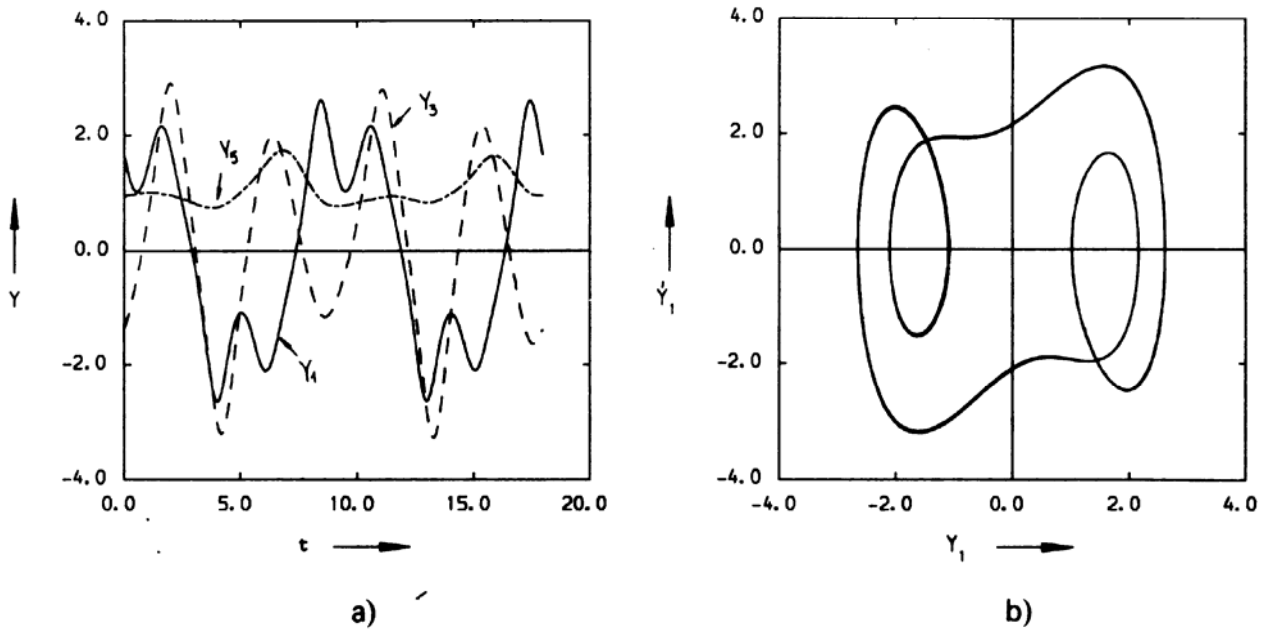

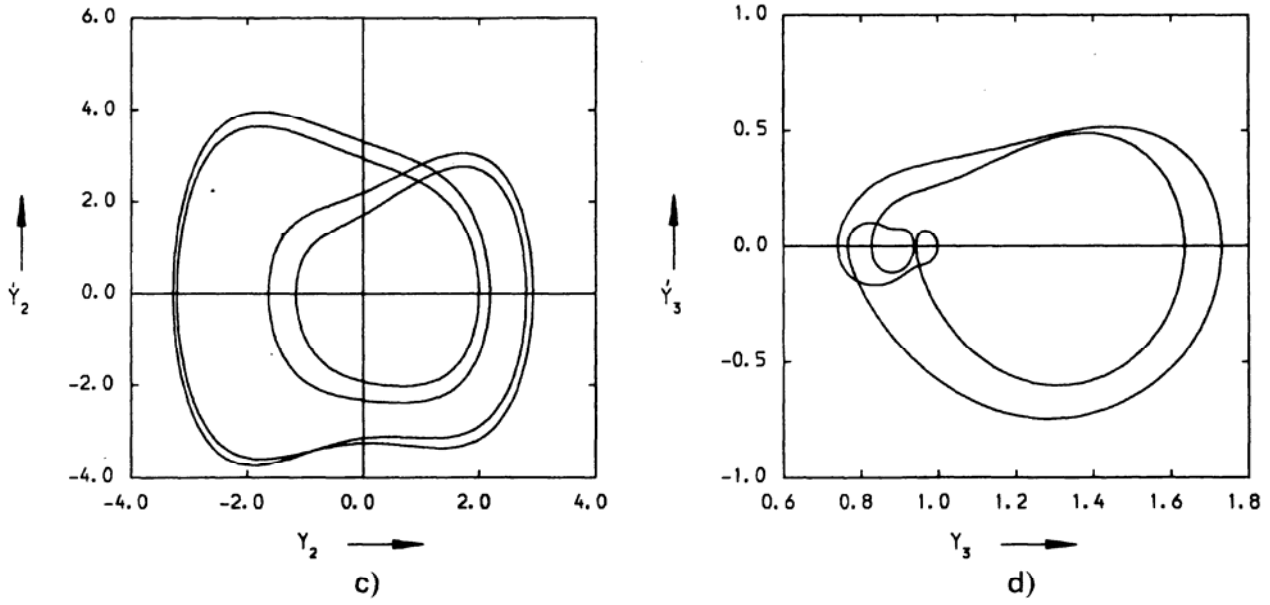

Fig. 4. Time histories (a)) and three projections of the double-periodic orbit (b), c), d)) found for $b = 0.02$

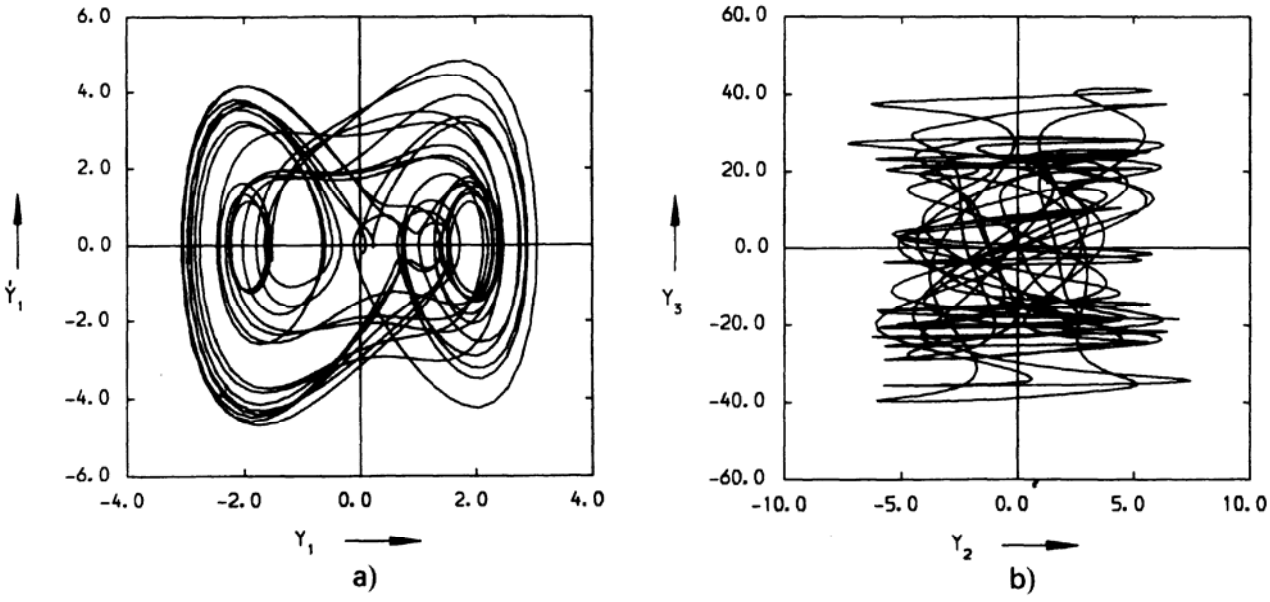

Fig. 5. a), b) Two projections of the strange chaotic attractor ($b = 0.1$)

loses its stability for $q = 4.429$, and a new stable periodic solution with the period $8\pi/\nu_0$ branches from it. The solution loses its stability already for $q = 4.41$ (one of the multipliers reaches the value of -1). A further decrease of q results in the increase of unstability of the solution, and for $q = 4.3292$ the projections of that unstable solution are presented in Fig. 8 (at that point one of the multipliers equals -16.58, and another is close to the value of $+1$). A further tracing of the cascade of bifurcation doubling the solution period has been found impossible on account of the branches of the newly created solutions to the branches of previous solutions. It is easily discernible from Fig. 6 that all

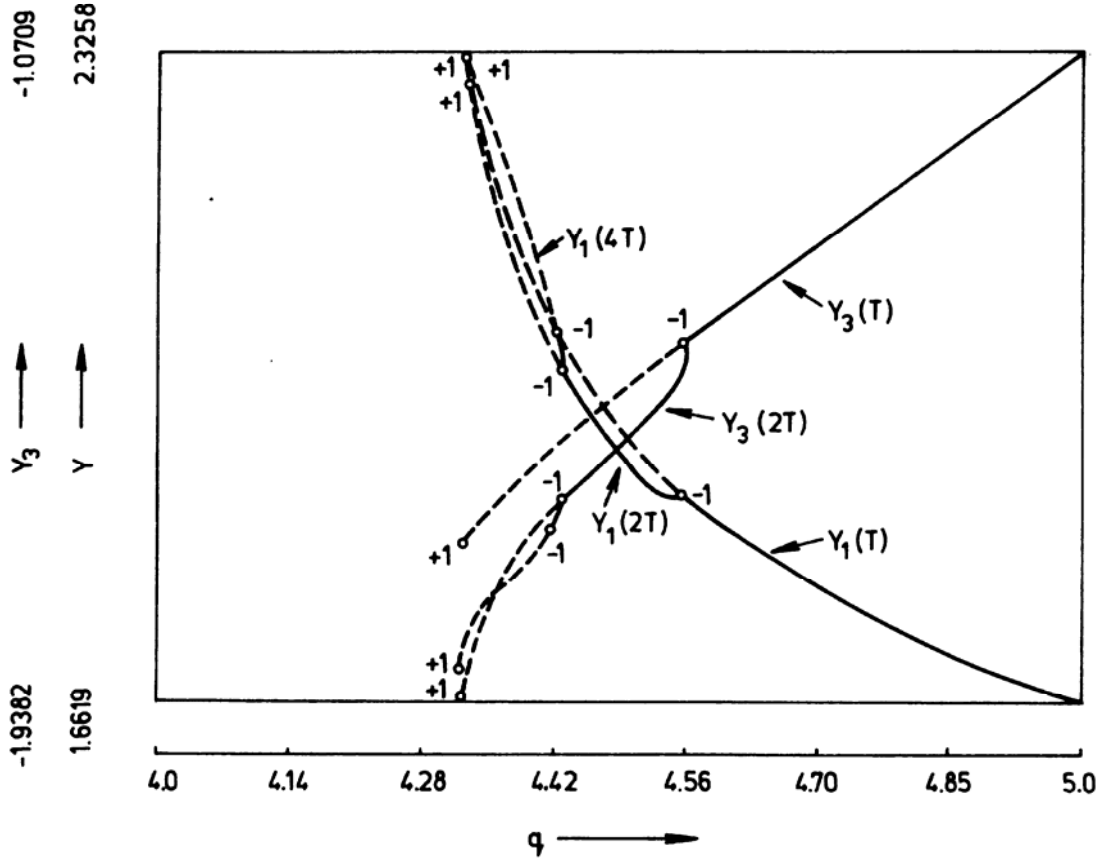

Fig. 6. Solution branches and bifurcation points of the periodic orbit against q

the three unstable branches of periodic solutions with the periods $2\pi/\nu_0$, $4\pi/\nu_0$ and $8\pi/\nu_0$ disappear for the same value of $q_{cr} = 4.3292$ (at that time one of the multipliers reaches the value of $+1$). For $q > q_{cr}$ a chaotic orbit appears with its exemplary projections for $q = 4.3$ presented in Fig. 9.

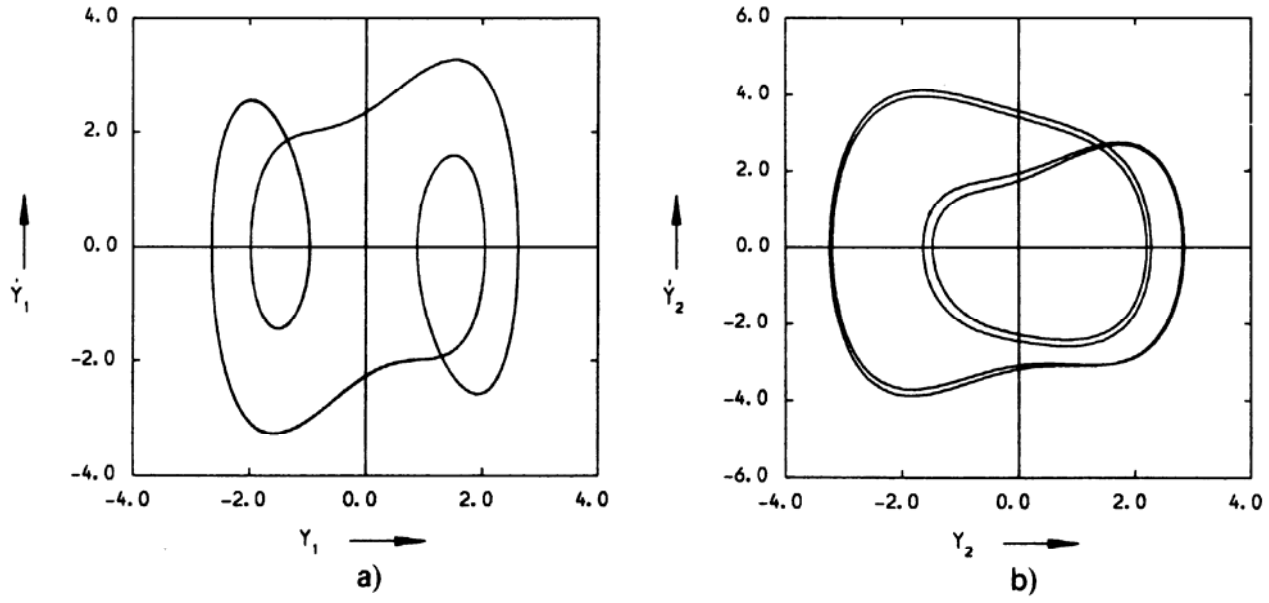

Fig. 7. a), b) Two projections of the doubled periodic orbit ($q = 4.53$)

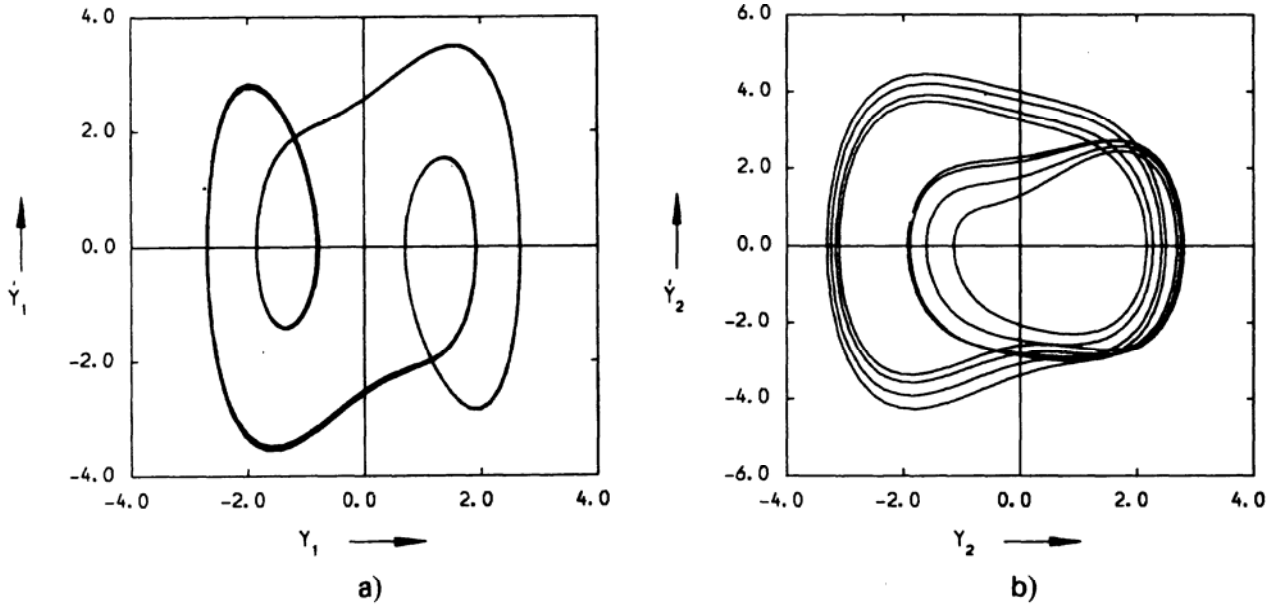

Fig. 8. Two projections of the triple periodic orbit ($q = 4.3292$)

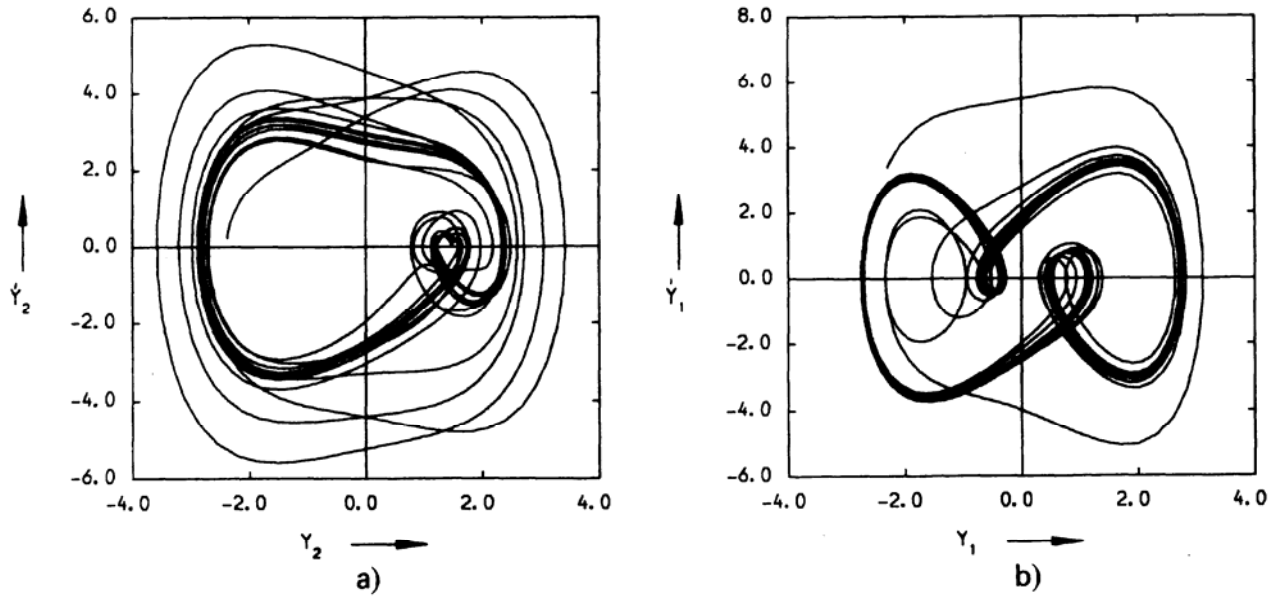

Fig. 9. a), b) Two projections of the strange chaotic attractor ($q = 4.3$)

5. Observation of chaos

In order to examine the chaotic behaviour of the analyzed system, a Poincarè map associated with equations (9) is used. This map or the (y_i, y_j) surface of section $\sum_{t_0}^{t_n} = \{\{y_i(t_n), y_j(t_n)\}, t_n = t_0 + 2\pi n v_0^{-1}\}$ is calculated by integrating equations (9). Additionally, the frequency power spectra (Fast Fourier Transform calculations) have been observed.

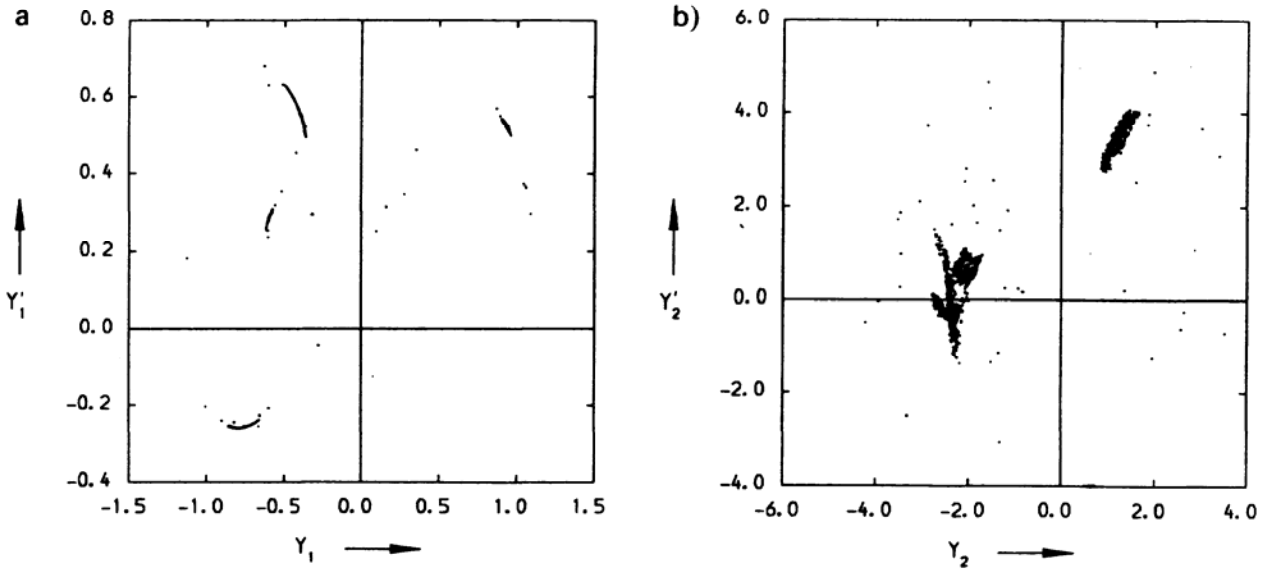

Fig. 10. Projections of the chaotic attractor (Poincarè map) onto the a): (y_1', y_1) and b): (y_2', y_2) planes

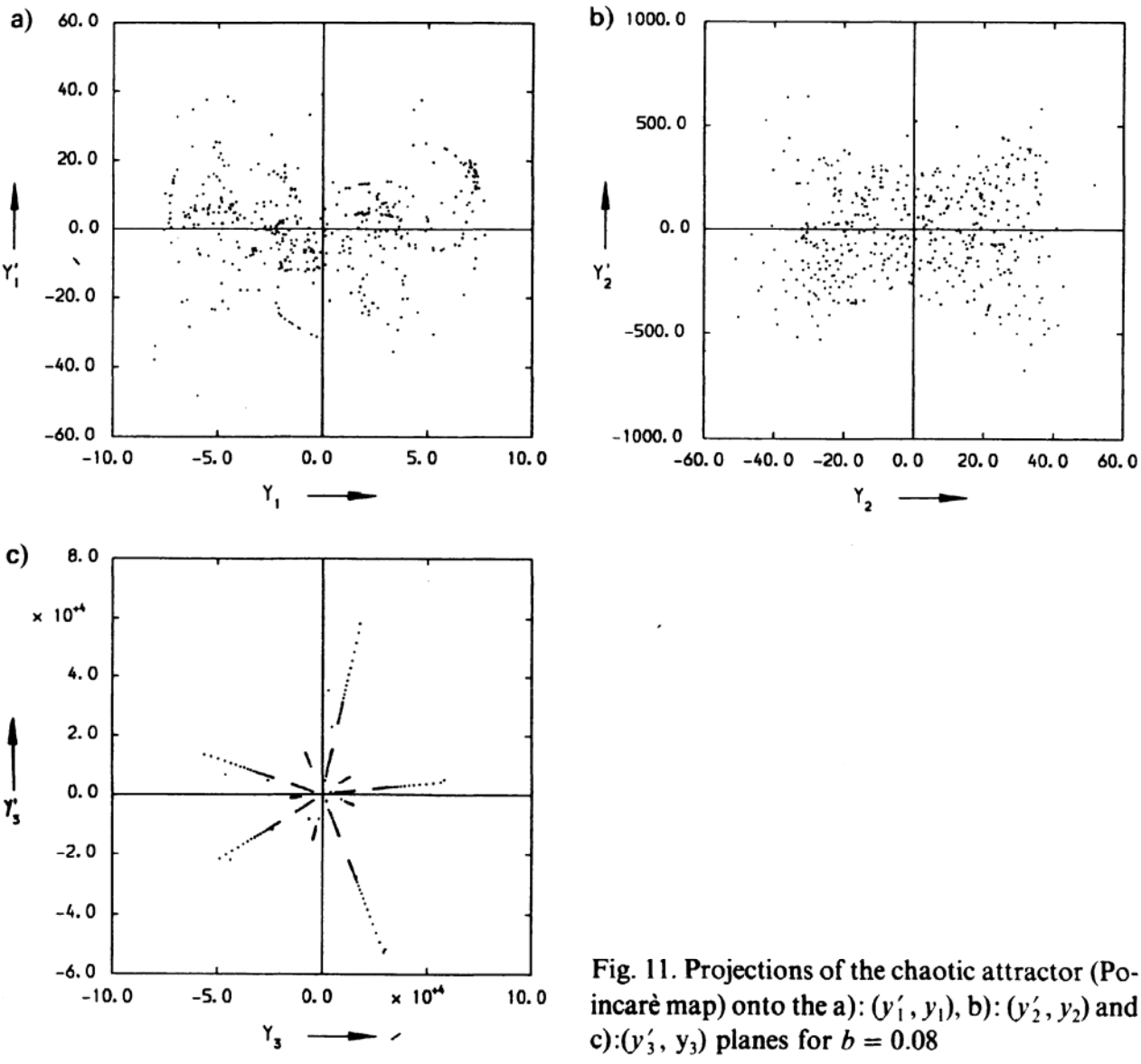

Fig. 11. Projections of the chaotic attractor (Poincarè map) onto the a): (y_1', y_1), b): (y_2', y_2) and c):(y_3', y_3) planes for $b = 0.08$

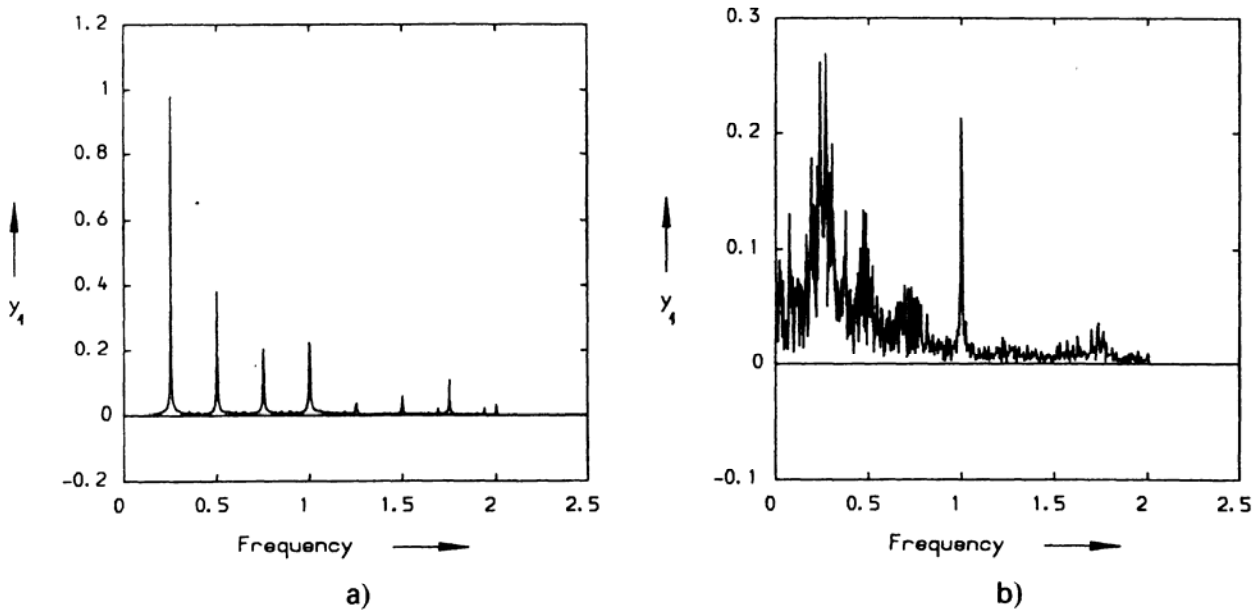

Fig. 12. Frequency power spectra for $y_1(\tau)$: a) $b = 10^{-5}$; b) $b = 0.08$

Numerical calculations have been made for the following parameters: $z = d_1 = d_2 = d_3 = \mu = 0.1$, $\nu = 0.8$, $\nu_0 = 1.0$, $q_1 = 0.15$, $q_2 = 0.0$, $r = \gamma = 0.5$, $E = 0.01$. If $b = 0$ then $\varepsilon = 0$ as well. This means that oscillations of $y_5(\tau)$ are regular. Chaotic oscillations of the concentrated mass m are presented in Fig. 10 which contains the Poincarè maps projections $y_1(y_1')$ and $y_2(y_2')$. With the increase of b the chaotic dynamics of the rotor also increases and chaotic oscillations are transferred on the coordinate $y_5(\tau)$. This is illustrated by Fig. 11, where Poincarè map is projected to three chosen planes in a similar way as before. If the projections presented in Fig. 11a, b indicate the strangness of the analyzed attractor, it is clearly seen that projections $y_3'(y_3)$ consists of points placed on sections of lines arranged radiantly. It is the result of compromise between the oscillations of the linear subsystem (rotor) in the y_3 direction, and the chaotic motions $y_1(\tau)$ and $y_2(\tau)$ coupled through b. The coupling increases with the increase of b. A certain hierarchy of chaotic motions can be noticed here. The travel of phase trajectories in the direction to the left and to the right of the origin of the coordinate system is several time faster for $y_1(\tau)$ than $y_2(\tau)$. The time history $y_3(\tau)$ consists of intervals of regular motions either increasing or decreasing in time with evident jumps between those intervals. The motion shows, however, a certain characteristic order, which is illustrated on the projection of $y_3'(y_3)$ map.

To the increase of chaotic dynamics of the system accompanying the increase of b testifies the change of frequency spectrum presented on the example of the coordinates $y_1(\tau)$ in Fig. 12.

6. Concluding remarks

The use of the shooting and Newton – Raphson methods has made it possible to trace the periodic orbit changes accompanying the change of two chosen parameters b and q in the dimensionless equation system (9). That equation system governs the oscillations of a mechanical system consisting of a rotor with different cross-section moments (parametric excitation) fixed in a harmonically--excited frame. It appears that in such a system it is possible to observe transitions to chaos never met in simple harmonically-excited oscillators, which have been so extensively discussed lately.

When analyzing the periodic orbit changes with the increase of b, after one of the multipliers has crossed the point -1 of the unit circle of the complex plane, it has been found that both the solutions (with periods $2\pi/\nu_0$ and $4\pi/\nu_0$) are unstable. For $b = 0.075$ one of the characteristic multipliers reaches the value of $+1$, and the further increase of b causes the appearance of the chaotic orbit.

In the second of the considered cases the decrease of the parameter q has been accompanied by three stages of the solution period doubling. A further numerical tracing of the cascade of bifurcation has been found impossible on account of the closeness of the bifurcation branches of the solutions. The calculations, however, have made it possible to discover another characteristic feature of the scenario leading to chaos. All the three branches of solutions which are unstable disappear simultaneously for a certain value of q_{cr}. For $q > q_{cr}$ a chaotic orbit appears.

Finally, a special kind of evolution of strange chaotic attractors with an increase of the control parameter b has been discussed and illustrated (a certain hierarchy of chaotic motions has been shown).

Acknowledgement

The numerical calculations were made in the Computation Center of the Technical University of Braunschweig during the author's stay in West Germany, under the terms of the Alexander von Humboldt Foundation scholarship. The authors would like to thanks to the reviewer for his valuable comments.

REFERENCES

[1] GUCKENHEIMER, J.—HOLMES, P. J.: Nonlinear oscillations, dynamical systems and bifurcations of vector fields. New York, Springer Verlag 1983. — [2] THOMPSON, J. M. T.—STEWART, H. B.: Nonlinear dynamic and chaos. Chichester, John Wiley and Sons 1986. — [3] MOON, F. C.: Chaotic vibrations. Wiley—Interscience 1987. — [4] SEYDEL, R.: From equilibrium to

chaos. Practical bifurcation and stability analysis. New York, Elsevier 1988. — [5] AWREJCEWICZ, J.: Two kinds of evolution of strange attractor for the example of a particular nonlinear oscillator. ZAMP, *40*, 1989. — [6] AWREJCEWICZ, J.: Three routes to chaos in simple sinusoidally driven oscillators. ZAMM, *70*, 1990. — [7] AWREJCEWICZ, J.: Gradual and sudden transition to chaos in a sinusoidally driven nonlinear oscillator. J. Phys. Soc. Jap., *58*, 1989, No 12. — [8] AWREJCEWICZ, J.: Bifurcation portrait of the oscillations of human vocal cords. J. Sound Vibr., *136* (1), 1990. — [9] AWREJCEWICZ, J.—DELFS, J.: Dynamics of self-excited stick-slip oscillator with two degrees of freedom. Part 2. Periodic and chaotic orbits. Europ. J. Mech. (to appear). — [10] AWREJCEWICZ, J.: Vibrations system: Rotor with self-excited support. Proc. Intern. Conf. Rotordyn. Tokyo 1986. — [11] HALL, G.—WATT, J.: Modern numerical methods for ordinary differential equations. Oxford, Clarendon Press 1976. — [12] ARNOLD, V. I.; Geometrical methods in the theory of ordinary differential equations. New York, Springer Verlag 1983.

Rukopis dodaný: 20. 3. 1990